Grzegorz GRALEWICZ, Grzegorz OWCZAREK,
Department of Personal Protective Equipment, Central Institute for Labour Protection – National Research Institute, Łódź
Bogusław WIĘCEK
Institute of Electronics, Technical University of Łódź

ANALYTICAL-NUMERICAL MODEL FOR THE DETECTION OF STRUCTURAL DEFECTS BY LOCK-IN THERMOGRAPHY

Keywords

Thermography, non-destructive evaluation, CFRP, structural defects, thermal parameters, geometric parameters.

Abstract

This paper presents the results of analytical-numerical modelling for the carbon-fibre-reinforced polymer (CFRP) structure using lock-in thermography. The method consists of the excitation of thermal effects in the tested structure caused by an external heat source. Simulations have been carried out to determine the optimum conditions for the lock-in evaluation in order to detect internal defects, measure their thickness and evaluate thermal properties. In the structure under study, a defect was simulated by inserting to the CFRP volume such materials as teflon and epoxy resin. Since many structures consist of CFRP, the rapid and remote identification of delaminations, impact damages and cracks is a topic of major concern.

The results of our study indicate that a method is required for the maintenance of safety relevant structures (e.g. aerospace equipment and vehicles) where one needs to defect areas early enough to prevent catastrophic failure.

Introduction

In lock-in thermography excitation can take the form of a single pulse of a pre-set duration or a series of pulses. Thermograms take measurements during the cooling and/or heating up. The response of the object to external excitation can be recorded directly on the stimulated surface (forward projection) or on the opposite surface, after the thermal wave has penetrated the object (back projection).

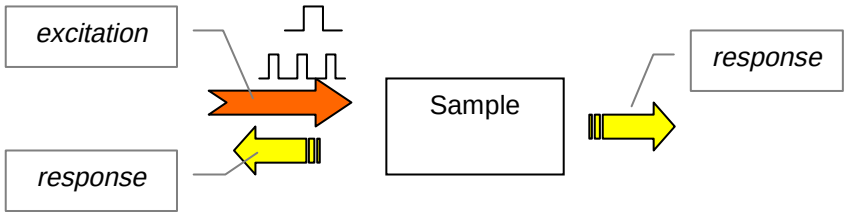

Fig. 1. Projection methods: forward and back

Thereafter, the Fourier transform of the response of the object to excitation is determined. A discrete Fourier transform is defined by the following relation [1]:

$$F\left(x_i, f\right)=\frac{1}{N}\Sigma_{n=1}^{N} S_n\left(x_i,t\right)\exp\left(-\frac{j2\pi ft}{N}\right)=\mathrm{Re}\left\{F\left(x_i, f\right)\right\}+ j\,\mathrm{Im}\left\{F\left(x_i, f\right)\right\} \quad (1)$$

where: Re(f) and Im(f) – real and imaginary parts of the Fourier transform of S_n images for each point x_i.

A series of amplitude images and phase images for any frequency are obtained. Amplitude images A(f) and phase images φ (f) are determined by the following relation [1]:

$$A(f)=\sqrt{\mathrm{Re}^2\left\{F\left(x_i, f\right)\right\}+\mathrm{Im}^2\left\{F\left(x_i, f\right)\right\}} \quad (2)$$

$$\varphi(f)=arctg\left(\frac{\mathrm{Im}\left\{F\left(x_i, f\right)\right\}}{\mathrm{Re}\left\{F\left(x_i, f\right)\right\}}\right) \quad (3)$$

Amplitude and phase values for individual points of the surface of the specimen make it possible to determine phase difference $\Delta\Phi$ between the homogenous (defect-free) area and the defected area [5]:

$$\Delta\Phi = \Phi_{defect} - \Phi_{without-defect} \tag{4}$$

In practice, the determination of phase difference allows for the detection of such defects in material structures as delamination, ruptures, air voids, etc. It is also possible to assess the boundaries of two types of material (geometric parameters).

The principle of measurement by this method is presented in Fig. 2. A computer-controlled thermal source ("thermal wave" generator) supplies energy to the specimen under study. The heat that penetrates the specimen and is disturbed in areas of material defects which is indicated by a modified distribution of the temperature field on the surface of the specimen. The process of heat penetration is synchronically recorded by a thermal camera in conditions of a pulsating source of heat. Measurement data is collected in computer memory and then analysed by special software.

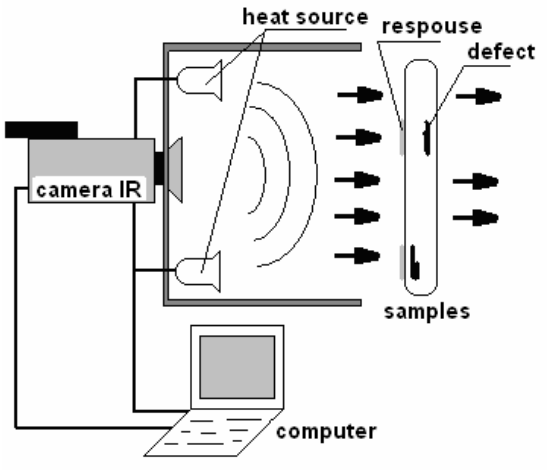

Fig. 2. Principle of measurement by lock-in thermography

The response of the object conveys information on a wide frequency spectrum, which allows analysing the heat penetration at various depths inside the specimen tested. Also important is that the method does not require repeated testing in order to evaluate various layers of the specimen.

The model testing was carried out both to determine optimal conditions for the lock-in evaluation and to determine limitations imposed by actual testing

conditions. The structure under study was characterized by much higher thermal conductivity than the materials representing the defect. This allowed the determination of the boundaries of applicability of the method. The effects of frequency and power of the excitation, depending on thermal and geometric parameters of the structure, were evaluated.

1. Structure under study

The model testing was carried out for the following material structure: carbon-fibre-reinforced polymer (CFRP). In this structure a defect was placed that was equivalent to delamination or voids. The defect was represented by teflon or epoxy resin. Thermal conductivity for these materials is significantly lower than for the base material (for teflon and resin k = 0.2 W m^{-1} K^{-1}, for CFRP k = 0.67 W m^{-1} K^{-1}).

The testing was first carried out for a homogenous (defect-free) structure, and then for a multilayer (defected) structure. The model of the structure assumes that two materials (defect) are characterized by significantly lower thermal conductivity than the base material (Table 1).

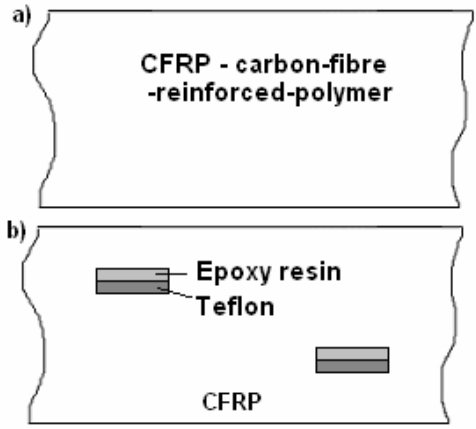

Fig. 3. Testing of structure: a) homogenous b) multilayer (defected)

The thickness of teflon was 0.6 mm, and the epoxy resin layer was 0.1 mm. The overall structure was 4 mm thick. The overall defect thickness was 0.7 mm. The defect was placed in depths from the surface of 0.3; 0.6, 1, 1.5, and 2 mm. The size of the structure was 300 mm x 300 mm x 4 mm.

To sum up, the defect-free structure is a homogenous plate 4 mm thick. The defected structure, on the other hand, is a four-layer plate: two layers of CFRP (above and below the defect), Teflon layer and resin layer (defect). The depth at

which individual layers were placed (for the defect situated at the depth of 0.3 mm) is $x_1 = 0.3$ mm, $x_2 = 0.4$ mm, $x_3 = 1.0$ mm, $x_4 = 4.0$ mm.

Table 1. Material Constants Used for Simulations

	Density ($kg\ m^{-3}$)	Thermal conductivity ($W\ m^{-1}\ K^{-1}$)	Specific heat ($J\ kg^{-1}\ K^{-1}$)
CFRP	1600	0.67	1200
Teflon	2150	0.209	1100
Epoxy resin	1300	0.2	1700

The assumptions made prior to starting the testing included the following: ambient temperature, 296.15 K thermal conductivity coefficient for the front (h_f) and back (h_r) surface are, respectively, 9 and 8 $W\ m^{-2}\ K^{-1}$. Thermal resistance between layers was assumed to be zero. The frequency of the source of heat was sinusoidal and kept within the range of 0.0037 to 1 Hz.

The mathematical-analytical model allows the modification of assumptions before commencement. The values assumed by authors were ambient temperatures and thermal diffusion coefficients that corresponded to laboratory conditions.

2. Analytical modelling

In the analytical model, it was assumed that a modulated thermal flux is applied to the front surface of the tested structure, according to this equation [6]:

$$Q = \left({}^{Q_0}\!/_{2} \right)[1 + \cos(\omega t)] \tag{5}$$

where: Q_0 – light intensity; ω – pulsation; t – time.

In each layer temperature diffuses according to the general equation of thermal conductivity:

$$\frac{\partial^2 T_i}{\partial^2 x} - \frac{\rho c}{k_i}\frac{\partial T_i}{\partial t} = 0 \qquad x_i \geq x \geq x_{(i-1)} \quad i = 1,\ldots,n \tag{6}$$

where T_i is the temperature in the *i* layer. Boundary conditions are as follows:

1) for the front surface:

$$-k_1\frac{\partial T_1}{\partial x}=\frac{Q_0}{2}\left[1+\cos(\omega t)\right]-h_f\left(T_f-T_\infty\right)=\mathrm{Re}\left(\frac{Q_0}{2}\left[1+\exp(j\omega t)\right]\right)-h_f\left(T_f-T_\infty\right)$$
$$x=0 \quad t>0 \tag{7}$$

2) the area of interaction between layers:

$$k_i\frac{\partial T_i}{\partial x}=k_{(i+1)}\frac{\partial T_{(i+1)}}{\partial x} \qquad x=x_i \;\; i=1,...,n-1 \;\; t>0 \tag{8}$$

$$T_{(i+1)}-T_i=R_{i,i+1}k_{(i+1)}\frac{\partial T_{(i+1)}}{\partial x} \qquad x=x_i \;\; i=1,...,n-1 \;\; t>0 \tag{9}$$

3) for the back surface:

$$-k_n\frac{\partial T_n}{\partial x}=h_r\left(T_r-T_\infty\right) \qquad x=x_n \qquad t>0 \tag{10}$$

The analytical solution to the general equation of thermal conductivity for *n* number of layers is as follows:

$$T_i(x,t)=T_{di}(x)+T_{ai}(x)\exp(j\omega t) \;\; i=1,...,n \tag{11}$$

where there are: dc (constant) component (T_{di}) and ac (variable) component (T_{ai}) of temperature for each of the layers.

As a result of further transformations presented by the authors in previous papers [5, 6], phase difference between the defected and defect-free areas has been obtained according to the equation (4).

Fig. 4 indicates that there are frequencies for defects present at some depth at which there is no phase difference or the phase difference is very small. This means that the defect cannot be detected at this particular excitation frequency. This frequency has been designated a “boundary frequency.” Also, two different frequencies can be observed at which the maximum positive and negative phase differences occur. These frequencies have been designated “optimum frequencies.” Obviously, at these frequencies of excitation the defect will be most detectable.

Fig. 4 illustrates the dependence of the “boundary” and “optimum” frequency on the depth at which the defect is located. One can see that the values of these frequencies decrease with the depth of the defect.

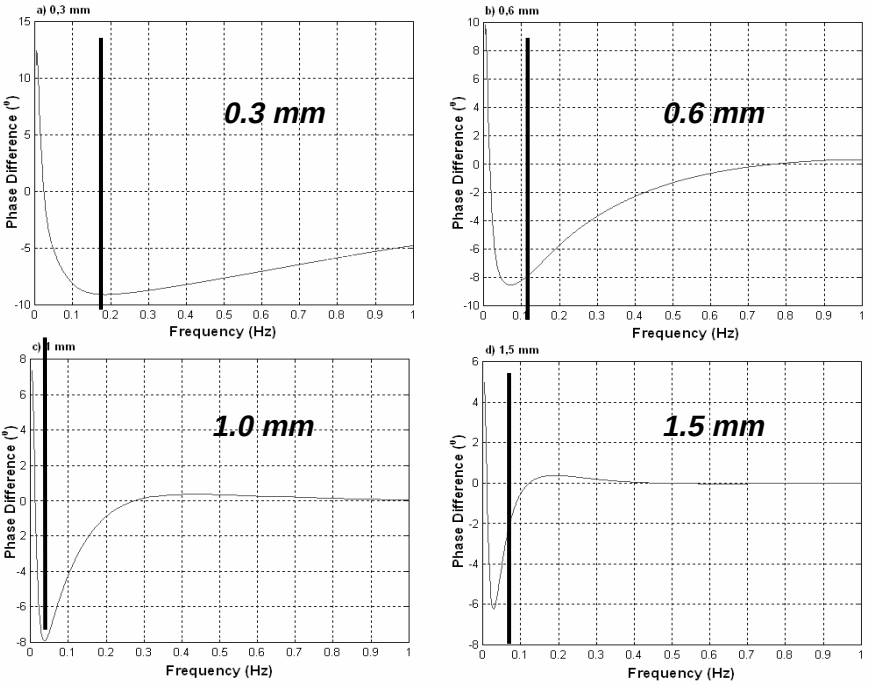

Fig. 4. Phase difference between the defected and homogenous structure for the defect located at the following depths: 0.3 mm, 0.6 mm, 1 mm, 1.5 mm

Based on the above results, it is possible to create a theoretical thermal model for the evaluated structure. This model can be used for predicting the "boundary" and "optimum" frequencies and is useful in choosing parameters for subsequent laboratory measurements of this structure, as well as when designing a measurement set-up.

The "optimum" and "boundary" frequencies for different depths of the defect location in the described thermal model for the tested structure are presented in Table 2.

Table 2. The values of "optimum" and "boundary" frequencies for different depths at which the defect is located – thermal model of the inspected structure

Depths	„Optimum" frequency	*„Boundary" Frequency*
x_1*[mm]*	*f [Hz]*	f [Hz]
0.3	0.19	*Over 9.4*
0.6	0.08	*Over 3.1*
1.0	0.05	*Over 0.9*
1.5	0.04	*Over 0.7*
2	*0.03*	*Over 0,3*

Based on the results presented in Table 2 the dependence of “optimum” and “boundary” frequencies as a function of the depth of location of the defect have been determined (Fig. 5 and 6).

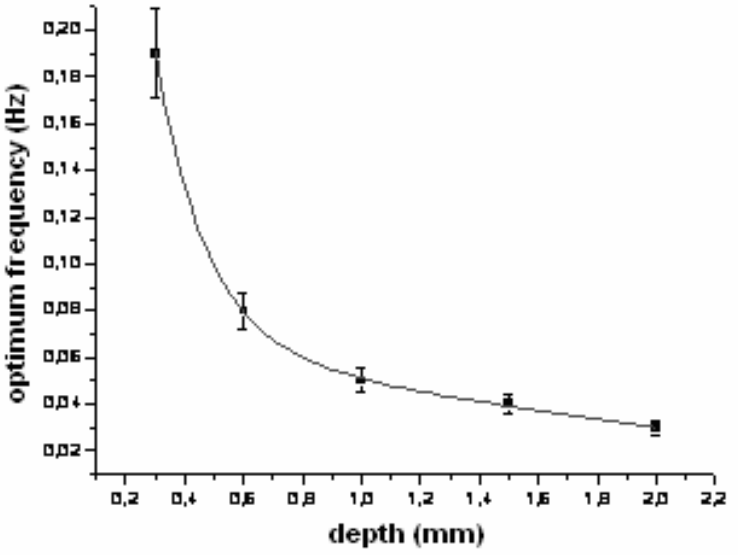

Fig. 5. The “optimum” frequency as function of the depth of location of the defect

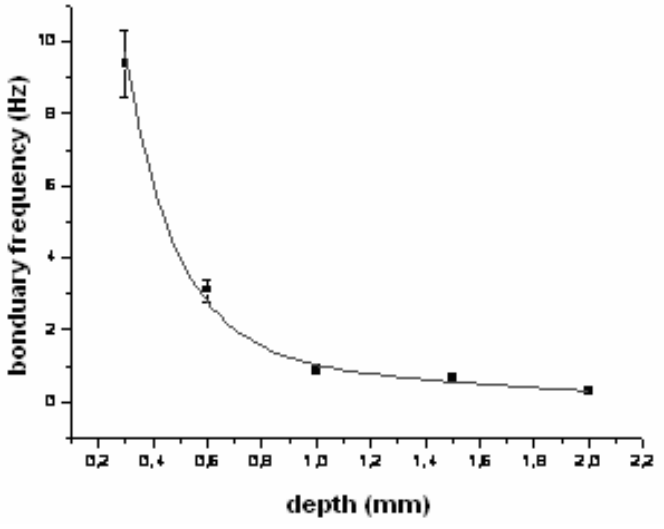

Fig. 6. The “boundary” frequency as function of depth of location of the defect

In both considered cases, i.e., for both the "optimum" and the "boundary" frequencies presented as function of depth of location of the defect, the relation is exponential. Very good matching of analytical functions to the optimum values from the modelling performed ($R^2 = 0.99$ for the "optimum" frequency as function of depth of the defect location; $R^2 = 0.97$ for the "boundary" frequency as function of the defect depth) allowed the determination of a "mathematical model," enabling, the determination of the "boundary" frequency for the defect located at specified depth.

3. Numerical modelling

Subsequent numerical modelling of the structure was carried out to determine the material boundaries for individual layers, which allowed the determination of the boundary parameters for material structures tested by the "thermal flux" method. Then, the relation between the depth of the defect location and temperature profile on the surface of the structure was studied.

To simplify and shorten the process of calculation, the structure dimensions of 4 mm x 0.01 mm were assumed, but other dimensions have not been changed. Fig. 7 presents a 4-layer structure for the defect placed at a depth of 0.3 mm from the surface.

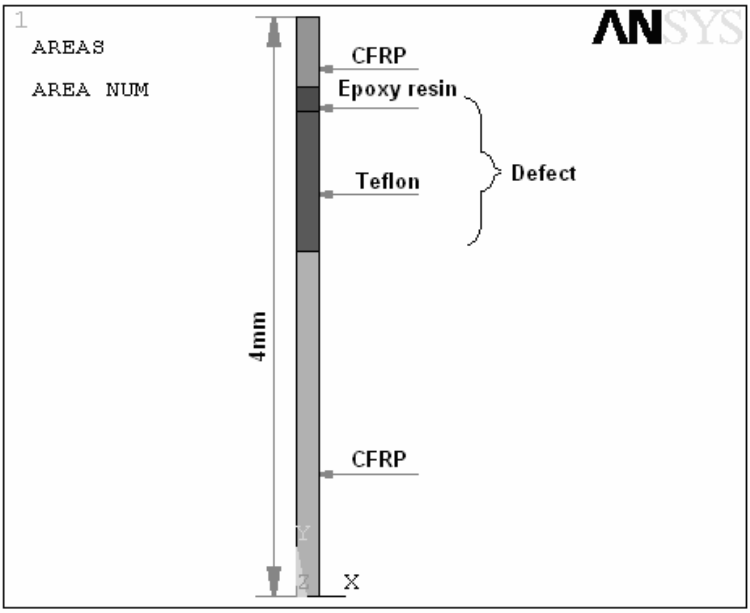

Fig. 7. 4-layer structure for the defect placed at the depth of 0.3 mm from the surface

The assumptions made prior to starting the testing include an ambient temperature 296.15 K and the thermal conductivity coefficient for the front and back surface are, respectively, 9 and 8 W m^{-2} K^{-1}. Stable temperatures are maintained on side surfaces of the structure. In this case the temperature field is single-dimensional.

Fig. 8 presents temperature changes on individual surfaces (CFRP, resin, Teflon, CFRP) of the structure as function of time. One can observe that the front surface is warming up to a temperature of 380 K, whereas the back surface warms up to 372 K at a thermal flux applied to the front surface of the structure, whose parameters correspond to the designed measurement set-up. The amplitude of temperature on the front surface is higher than on the back. On the back surface the amplitude has almost ceased.

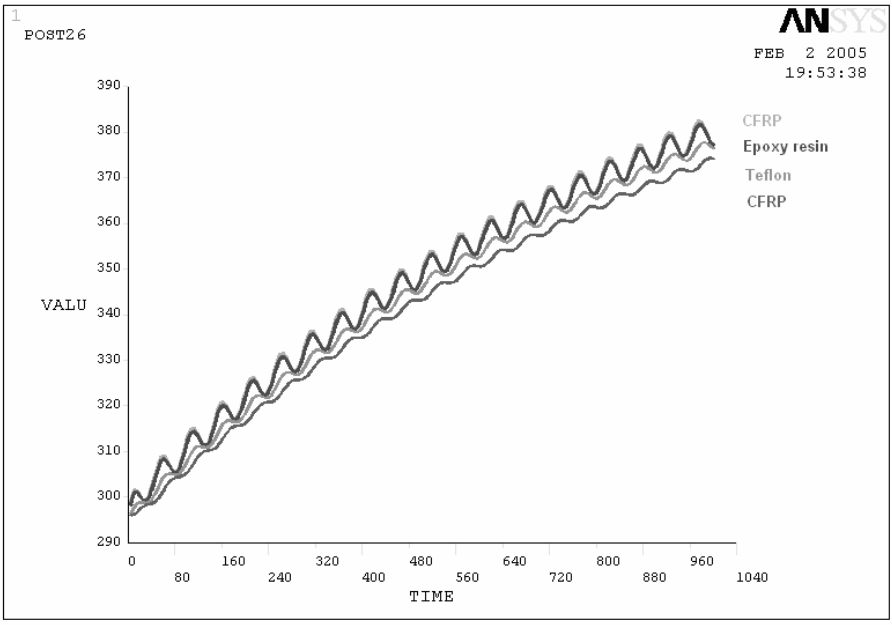

Fig. 8. Temperature changes on individual surfaces of the tested structure as function of time for an excitation frequency of f=1Hz and t_end=1000s (for the transient state)

As the input excitation is sinusoidal and temperature changes inside the structure are also sinusoidal, with a correspondingly damped amplitude. The farther from the surface, the lower is the amplitude of temperature.

Using an application compiled in Matlab, the amplitude of temperature and mean temperature for Ansys-based results were determined, for the testing carried out at excitation frequency of f = 1 Hz and duration of 1.000 s. The farther from the surface, the more dampened the amplitude of the temperature.

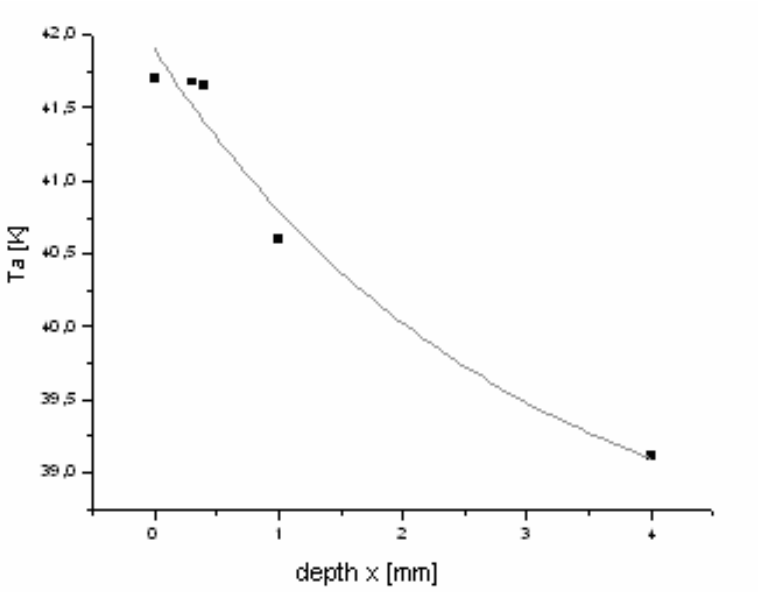

Fig. 9. Temperature amplitude changes as function of depth for the frequency of the excitation f=1Hz, duration=1000 s

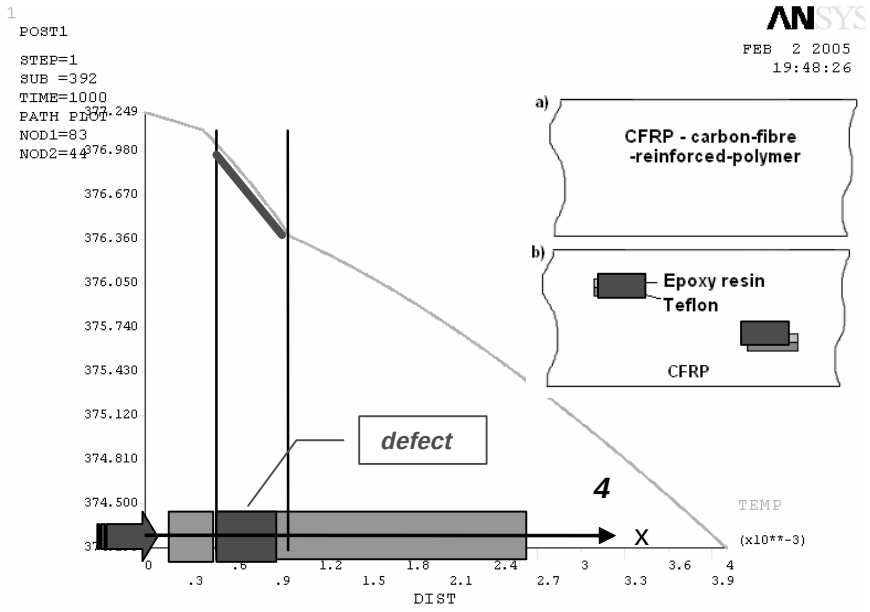

Fig. 10. Changes of a mean temperature as function of depth for the frequency of the excitation f=1Hz, duration=1000 s

Changes of mean temperature as a function of depth (Fig. 10) indicate the location of the defect. Straight lines of different slopes and lengths, depending on thermal parameters of the layer thickness represent all layers.

a)

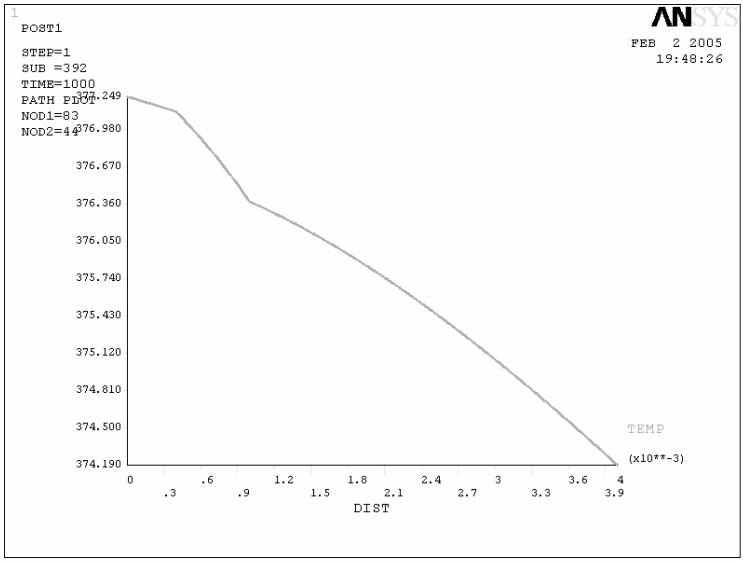

b)

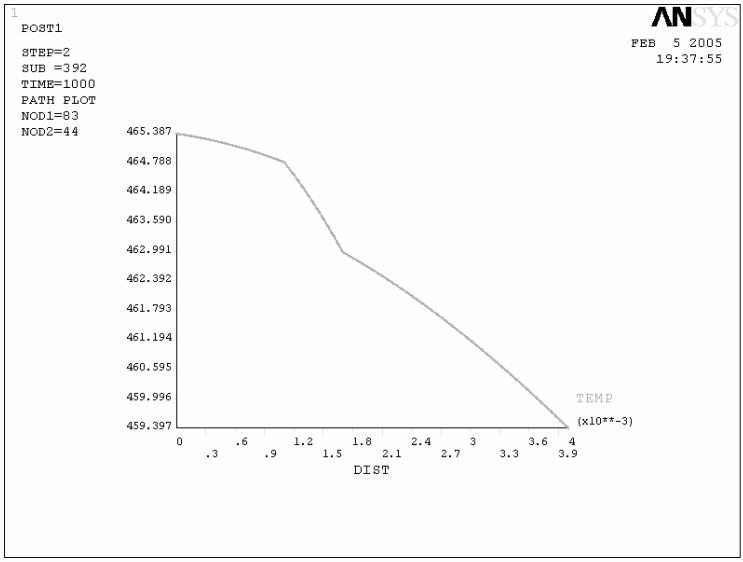

c)

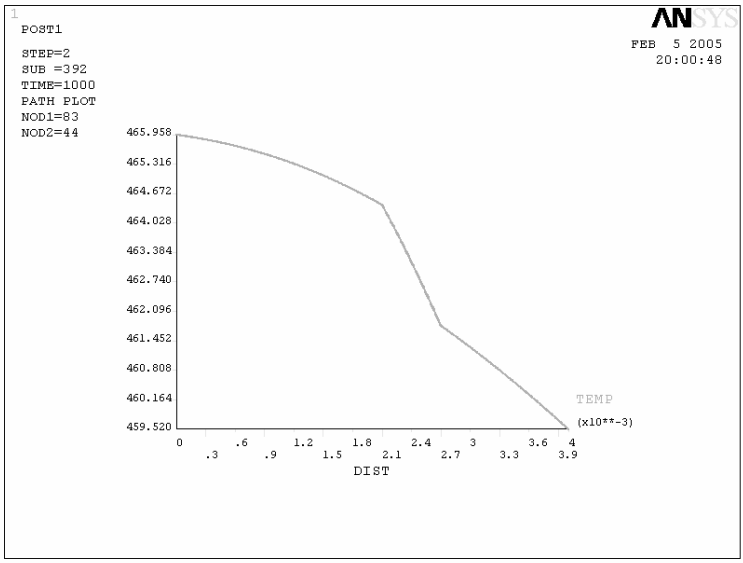

Fig. 11. Temperature change as function of depth for the defect located at depths of a) 0.3 mm, b) 1 mm, and c) 2 mm from the surface

To confirm the character of temperature changes, further modelling was carried out using the Ansys package. Fig. 11 presents temperature changes as a function of depth for the defect located 0.3 mm from the surface. The spot of the defect is seen. Each of the layers that represent the defect has a different slope and length (as above). This makes the defect detectable and its location identifiable. The shape of modulation depends on material parameters and thickness of subsequent layers. The thermal conduction coefficient k of a layer and boundary parameters have a very large impact on this shape. When moved from 0.3 mm to 2 mm of the surface, the defect was still detectable.

Conclusions

The conclusions of the analytical-numerical modelling presented in the paper are as follows:

- Active thermography can be used for the detection of internal defects, while carrying out of measurements of layer thickness, as well as evaluation of thermal properties of material structures.
- The lower the frequencies are of the heat pulse, the higher are the amplitudes of temperature; thus, lower frequencies better penetrate the inspected structure.

- The farther from the surface of the structure, the lower is the amplitude of temperature.
- Changes of mean temperature as a function of depth indicate the location of the defect. All layers are represented by straight lines of different slopes and lengths, depending on thermal parameters of the layer thickness.
- The depth of penetration decreases with the increase of the frequency of the thermal wave and the reduction of duration of the pulse. It also depends on the material (k, ρ, c_w). Therefore, by knowing at least the approximate thickness of the inspected layers, it is possible to select an appropriate duration of the excitation pulse and/or frequency of the sine excitation curve.
- Appropriate selection of the power of the thermal wave is one of more important factors in localization of defects. It is essential to align the power of the pulse to the test material, for when boundary values are exceeded damage of the inspected structure may result.

The results of analytical-numerical modelling show that the method is applicable for non-destructive inspection of structures where it can detect impact, delamination and crack. Therefore, a method is required that is applicable during the inspection procedure to monitor the integrity of such structures.

Acknowledgements

Scientific work carried out within the project "Development of high-tech products and devices" in The Multi-Year Programme entitled "Development of innovativeness systems of manufacturing and maintenance 2004-2008."

References

1. Nowakowski A.: Postępy termografii – aplikacje medyczne. Wydział Elektroniki, Telekomunikacji i Informatyki Katedra Elektroniki Medycznej i Ekologicznej Gdańsk – 2001.
2. Więcek B., Zwolenik S.: Zastosowanie termografii w badaniach nieniszczących metoda fali cieplnej, termografia impulsowa. Instytut Elektroniki Politechniki Łódzkiej.
3. Rudowski G.: Termowizja i jej zastosowanie. Wydawnictwa Komunikacji i Łączności – Warszawa 1978.
4. Gralewicz G., Więcek B., Owczarek G.: Zastosowanie termografii w badaniach nieniszczących. Zeszyty Elektroniki, Politechnika Łódzka, 01.2005, p. 31-61.

5. Gralewicz G., Owczarek G., Więcek B.: Investigations of Single and Multilayer Structures Using Lock-In Thermography - Possible Applications, International Journal of Occupational Safety and Ergonomics (JOSE) 2005, Vol. 11, No. 2, 211–215.
6. Owczarek G., Gralewicz G.: Lokalizacja defektów materiałowych z wykorzystaniem promieniowania podczerwonego – monografia, 2003, CIOP – PIB, Warszawa, Poland.
7. Gralewicz G., Owczarek G., Więcek B: Wykrywanie korozji - metoda badan nieniszczących w podczerwieni. Ochrona przed korozją 12/2004, p. 1-5.

Reviewer:
Krzysztof ZDUNEK

Model analityczno-numeryczny wykrywania defektów strukturalnych metodą termografii synchronicznej

Słowa kluczowe

Termografia, badania nieniszczące, CFRP, defekty strukturalne, parametry cieplne, parametry geometryczne.

Streszczenie

W pracy przedstawiono wyniki modelowania analityczno-numerycznego dla struktury karbon-włókno-wzmocniony polimer (CFRP) wykorzystując metodę termografii synchronicznej (lock-in). Metoda ta polega na wymuszaniu przez zewnętrzne źródło ciepła zjawisk termicznych zachodzących w badanej strukturze. Przeprowadzone symulacje miały na celu określenie optymalnych warunków badań metodą lock-in, w celu wykrywania defektów wewnętrznych, dokonywania pomiaru grubości ich warstw, a także badania właściwości cieplnych. W analizowanej strukturze defekt był symulowany przez wprowadzenie do objętości CFRP takich materiałów, jak teflon i żywica epoksydowa.

Wyniki przedstawione w pracy potwierdzają przydatność metody przy ocenie struktur materiałowych (wykorzystywanych w lotnictwie oraz przemyśle samochodowym), gdzie odpowiednio wcześnie wykryte defekty struktur mogą zapobiec groźnym wypadkom.